

## Comparison of the Mechanism and Kinetics of Living Carbocationic Isobutylene and Styrene Polymerizations Based on Real-Time FTIR Monitoring<sup>†</sup>

Judit E. Puskas,\* Sohel Shaikh

Macromolecular Engineering Research Centre, Department of Chemical and Biochemical Engineering, The University of Western Ontario, London, Canada N6A 5B9

E-mail: jpuskas@uwo.ca

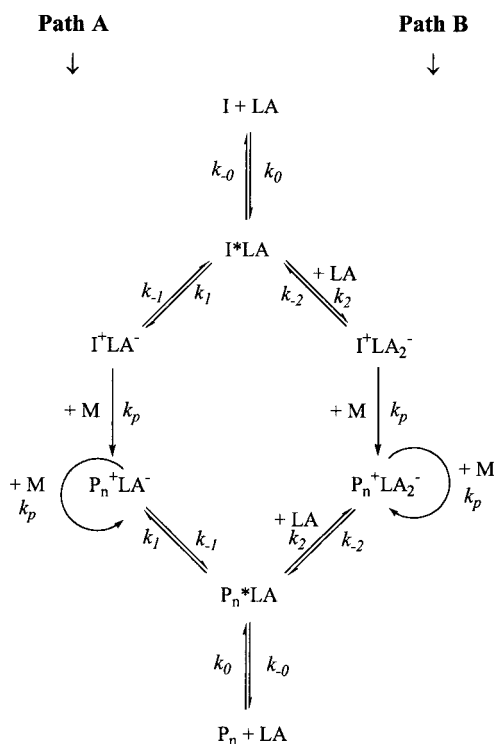
**Summary:** This paper will compare the mechanism and kinetics of living carbocationic polymerization of isobutylene (IB) and styrene (St), initiated by the 2-chloro-2,4,4-trimethyl-pentane (TMPCl) /  $\text{TiCl}_4$  system in 60/40 (v/v) methylcyclohexane / methyl chloride mixed solvent at  $-80$  and  $-75$  °C. The rate of initiation was found to be first order in  $\text{TiCl}_4$  in both systems. While initiation is instantaneous in IB polymerization at  $[\text{TiCl}_4]_0 \geq [\text{TMPCl}]_0$ , it is slow in St polymerization. Kinetic derivation showed that initiating efficiency is dependent on  $[\text{M}]$  in this latter system, which was also demonstrated experimentally. The apparent initiation rate constant was determined from initiator consumption rate data and was found to be  $k_{i,\text{app}} = 1.39 \text{ l}^2/\text{mol}^2\text{sec}$ . The rate of St consumption measured using a real time fibre-optic mid-FTIR monitoring technique compared well with gravimetric data and was found to be closer to first order in  $\text{TiCl}_4$  at  $[\text{TiCl}_4]_0 < [\text{TMPCl}]_0$ . However, the rate followed a close to second order in  $\text{TiCl}_4$  at  $[\text{TiCl}_4]_0 \geq [\text{TMPCl}]_0$ . The mechanistic model proposed earlier for living carbocationic IB polymerization, which yielded good agreement with experimental data, seems to apply to carbocationic St polymerization as well. This model reconciles the discrepancy between rate constants published for carbocationic IB and St polymerizations, and accounts for shifting  $\text{TiCl}_4$  orders. However, independent investigations are necessary to verify the proposed mechanistic model. Optimized conditions led to living carbocationic St polymerization producing high molecular weight PS with 100% initiating efficiency.

**Keywords:** cationic polymerization; kinetics; mechanism; polyisobutylene; polystyrene; real time FTIR

<sup>†</sup>This paper is dedicated to the memory of Dr. Michael Lanzendörfer.

## Introduction

Living polymerization has been at the frontiers of research in recent years. Living polymerizations have no side reactions such as irreversible termination and chain transfer, and provide great control over the polymerization process<sup>1</sup>. While living anionic polymerizations have been researched extensively and are commercialized, living carbocationic and radical polymerizations are relatively new<sup>2</sup>. Living carbocationic polymerization, the primary interest of our research group, is believed to be a more complex system than the classical living anionic polymerization<sup>2</sup>. The design and effective synthesis of various polymeric structures such as blocks, grafts, stars and arborescent (hyperbranched) polymers require thorough understanding of the mechanism of the polymerization process. Furthermore, optimization of the process conditions needs kinetic understanding. Our group has been investigating the mechanism and kinetics of living carbocationic polymerizations, and has proposed a comprehensive mechanism for living isobutylene (IB) polymerization initiated by 2,4,4-trimethyl pentyl chloride (TMPCl)/TiCl<sub>4</sub><sup>3</sup>. TMPCl was used as a model for the growing chain end thus the rates of initiation and propagation were considered to be equal. In this model, two reaction pathways (Path A and Path B) proceed in competition as shown in Scheme 1. Although the existence of the polymerization-inactive complexes I\*LA and P<sub>n</sub>\*LA has not been demonstrated experimentally, this model consolidated experimental evidence that the reaction order in TiCl<sub>4</sub> can shift between first and second order<sup>3-12</sup>. According to this mechanism, both pathways may proceed simultaneously, depending on the actual [TiCl<sub>4</sub>] concentration. The existence of Path A has been demonstrated experimentally: using [TMPCl]<sub>0</sub> > [TiCl<sub>4</sub>]<sub>0</sub> conditions were created under which Path A was shown to dominate the process<sup>3,6,9,12</sup>. The mechanism presented in Scheme 1 has been debated, which prompted us to further investigate this model, and compare it with other models. In addition, we intended to investigate the kinetics and mechanism of carbocationic styrene (St) polymerizations, in comparison with our model living IB polymerization.



Scheme 1: Proposed comprehensive mechanism for living IB polymerization<sup>3</sup>.

This paper will discuss some aspects of the mechanism and kinetics of living IB polymerization. It will also investigate the kinetics and mechanism of carbocationic St polymerizations initiated by the TMPCl/TiCl<sub>4</sub> system, and compare them with the kinetics and mechanism of carbocationic IB polymerization.

## Experimental

### Materials

2-chloro-2,4,4-trimethyl-pentane (TMPCl) was synthesized by HCl addition to 2,4,4-trimethyl-1-pentene<sup>12</sup>, and its purity was checked by <sup>1</sup>H NMR. TiCl<sub>4</sub>, dimethyl acetamide (DMA), *Dt*BP (2,6-di-*tert*.-butylpyridine) and methanol were used as received (Aldrich). Methyl chloride (MeCl, BOC gases) was dried by passing it through a column filled with BaO and CaCl<sub>2</sub>. Hexane (Hx) and methylcyclohexane (MeCHx) were refluxed with CaH<sub>2</sub> for at least 24 hours and distilled freshly before use. Styrene (St, Aldrich) was purified by vacuum distillation before use.

### Procedures

*Polymerizations.* The polymerizations were carried out in an MBraun LabMaster 130 glove box equipped with an integral cold hexane bath under dry nitrogen at -78<sup>0</sup>C, as reported earlier for IB polymerizations<sup>3,12</sup>.

*IR Monitoring.* The polymerization reactions were monitored in real time using a low temperature fiber-optic probe equipped with a transmission (TR) head<sup>5</sup>. The IR probe (Remspec Inc.), with its source and receiver cables, was interfaced with a Bio-Rad FTS 175C FTIR unit, to which a mid-IR fiber-optic liquid nitrogen cooled 0.5 x 0.5 mm MCT detector was attached. The cable bundle was fed into the glove box through a port, and the probe was immersed into the reactor. FTIR data were analyzed as reported earlier<sup>6</sup>.

*Polymer Characterization.* Polymer molecular weights (MWs) and molecular weight distributions (MWDs) were determined by Size Exclusion Chromatography (SEC) using a Waters system as described earlier<sup>6</sup>. The ASTRA (Wyatt Technology) software was used to obtain absolute MW data with dn/dc=0.183 ml/g for polystyrene (PS) in THF.

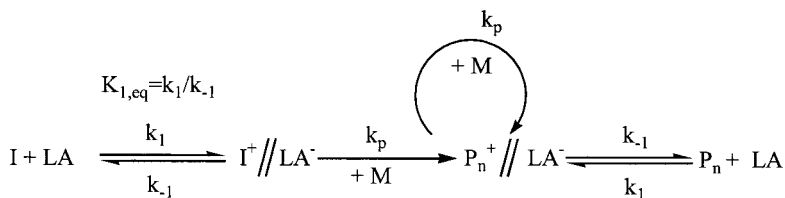
## Results and Discussion

### Living carbocationic IB polymerization

#### *Mechanistic models*

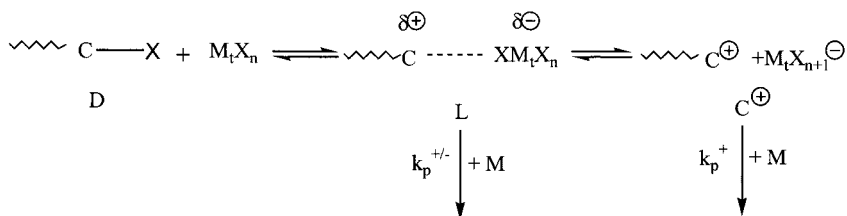
Living IB polymerization is governed by a dynamic equilibrium between covalent and ionic species, with the equilibrium strongly shifted towards the former. Several mechanistic models were proposed to describe this system. Our first model is shown in Scheme 2. This model

was developed for IB polymerization initiated by  $\text{TMPCl/TiCl}_4$ , which we consider a model system as the structure of the initiator resembles that of the growing PIB chain. In this model,  $\text{I}_n^+//\text{LA}^-$  and  $\text{P}_n^+//\text{LA}^-$  were shown to be ion pairs.



Scheme 2: Model of living IB polymerization initiated by  $\text{TMPCl/TiCl}_4$ .<sup>12,13</sup>

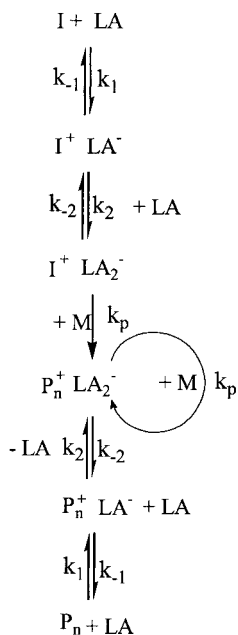
Majoros and Nagy from the Kennedy group developed a closed-loop comprehensive model using the Winstein ionicity spectrum, shown in Scheme 3:



Scheme 3: Comprehensive closed-loop mechanism by Majoros *et al.*<sup>4</sup>

where D represents a "dormant cationogen" (initiator or polymer), L stands for a sub-spectrum of polarized (stretched or activated, more-covalent-than-ionic) dipole intermediates leading to living polymerization, and C summarizes a further sub-spectrum of ionized entities starting with contact ion pairs through solvent separated ion pairs to fully solvated "free" ion pairs. These authors proposed that L and C can both initiate polymerization, but only L will lead to living conditions.

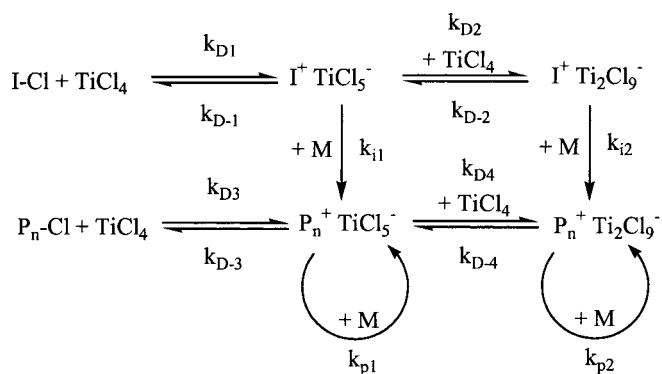
The reaction mechanism shown in Scheme 4 is based on the model of living IB polymerization proposed by Storey's group<sup>8</sup>.



Scheme 4: Mechanism of living IB polymerization based on a model proposed by Storey and Choate<sup>8</sup>.

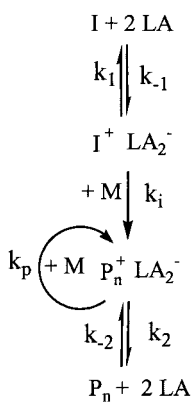
These authors suggested that propagation takes place predominantly through chains possessing dimeric gegenions which form by the reaction of additional  $\text{TiCl}_4$  with monomeric gegenions, as opposed to direct ionization by neutral, dimeric  $\text{Ti}_2\text{Cl}_8$ . They also presented kinetic derivation that direct ionization by neutral, dimeric  $\text{Ti}_2\text{Cl}_8$  would lead to first order dependence in  $[\text{TiCl}_4]$ , which would have been in direct contradiction with their experimental results.

The same group later proposed another model; the mechanistic pathway based on this is presented in Scheme 5. This work also reported propagation predominantly by active centers with dimeric gegenions.



Scheme 5: Mechanism of living IB polymerization based on the model proposed by Storey and Donnalley<sup>11</sup>.

Based on the work of Faust *et al.*,<sup>10, 14-15</sup> the following mechanism can be presented, as shown in Scheme 6:



Scheme 6: Model of living IB polymerization based on the work of Faust *et al.*<sup>10</sup>

The mechanistic models proposed in Schemes 1-6 all agree in the existence of dynamic equilibria between dormant and active species, and that only a fraction of the initiator and polymer chains is ionized at any given time. However, there is disagreement in the mechanism of initiation and propagation. The next section will compare these models based on kinetic investigations.

### Kinetics and rate constants

As mentioned above, living IB polymerization initiated by TMPCl/TiCl<sub>4</sub> can be considered as a model system, because the structure of the TMPCl initiator resembles the structure of the growing chain. Thus in the first model shown in Scheme 2 it was assumed that  $k_i = k_p$ , which greatly simplified the kinetic derivations<sup>12</sup>. The conversion dependence of the molecular weight distribution (MWD) in this system was described using the following equation.

$$\frac{DP_w}{DP_n} = 1 + \frac{(2\bar{l} - 1)}{DP_n} = 1 + \frac{\bar{l}_0}{DP_n} \quad (1)$$

where  $\bar{l} = (k_p/k_{-1})[M]$  and  $\bar{l}_0 = \bar{l}$  at  $[M]_0$ . From experimental MWD-conversion data  $k_p/k_{-1} = 16.5$  l/mol was calculated<sup>13</sup>. A similar treatment was later published by Müller *et al.*<sup>16</sup>. Roth and Mayr subsequently measured  $k_p = 6 \pm 2 \times 10^8$  l/molsec using the “diffusion clock” method<sup>17</sup>. Schlaad *et al.* recently published  $k_p = 7 \times 10^8$  l/molsec, also obtained from competition experiments<sup>14</sup>. These high values agree with industrial experience. In contrast,  $k_p$  values obtained from kinetic measurements are several orders of magnitude lower (see Table 1), with the exception of  $k_p$  measured in irradiation-induced IB polymerization in bulk<sup>23</sup>. This discrepancy was discussed by Plesch<sup>22, 24</sup> and remains a problem.

Table 1:  $k_p$  values in carbocationic IB polymerizations obtained by various methods

$k_p$ (l.mol <sup>-1</sup> s <sup>-1</sup> )	Initiating system	Solvent	T / °C	Ref.
$6 \times 10^3$	AlBr <sub>3</sub> / TiCl <sub>4</sub>	heptane	-14	18
$7.9 \times 10^5$	Light / VCl <sub>4</sub>	in bulk	-20	19
$1.2 \times 10^4$	Et <sub>2</sub> AlCl/Cl <sub>2</sub>	CH <sub>3</sub> Cl	-48	20
$9.1 \times 10^3$	Ionizing radiation	CH <sub>2</sub> Cl <sub>2</sub>	-78	21, 22
$1.5 \times 10^8$	Ionizing radiation	in bulk	-78	23
$6 \times 10^8$	R-Cl / TiCl <sub>4</sub>	CH <sub>2</sub> Cl <sub>2</sub>	-78	17*
$7 \times 10^8$	IB 33-mer / TiCl <sub>4</sub>	Hexanes / CH <sub>3</sub> Cl	-80	14*

\* Diffusion clock / competition experiments

Using  $k_p = 6 \times 10^8$  l.mol<sup>-1</sup>sec<sup>-1</sup> Puskas and Peng<sup>7</sup> calculated  $k_{-1} = 3.9 \times 10^7$  sec<sup>-1</sup>. Based on the model shown in Scheme 2,  $k_1 = 0.22$  l.mol<sup>-1</sup>sec<sup>-1</sup> was obtained from experimental initiator consumption data<sup>3</sup>. These rate constants were then used to simulate experimental data with the Predici software



developed for polymerization kinetic modelling<sup>25</sup>, and good agreement was found between simulated and experimental data<sup>7</sup>. However, the model in Scheme 2 does not reflect the experimental fact that living IB polymerization usually exhibits close to second order in  $[\text{TiCl}_4]$ . The model shown in Scheme 1 was proposed to accommodate the fractional and shifting  $\text{TiCl}_4$  orders found experimentally in living IB polymerizations. Using this model, the following composite rate constants were obtained from experimental data:  $K_0k_i = 0.22 \text{ l mol}^{-1}\text{sec}^{-1}$  from initiator consumption data and  $K_0K_1k_p = 3.4 \text{ l}^2 \text{ mol}^{-2}\text{sec}^{-1}$  from monomer consumption data in Path A, and  $K_0K_2k_p = 52 \text{ l}^3 \text{ mol}^{-3}\text{sec}^{-1}$  from monomer consumption data in Path B. Initiator consumption data cannot be measured experimentally in Path B as initiation practically is instantaneous. With  $k_p = 6 \times 10^8 \text{ l mol}^{-1}\text{sec}^{-1}$  we calculated  $K_0K_1 = 5.7 \times 10^{-9} \text{ l mol}^{-1}$  and  $K_0K_2 = 8.7 \times 10^{-8} \text{ l}^2 \text{ mol}^{-2}$ . Individual rate constants were obtained by parameter estimation using the model in Scheme 1 and experimental data<sup>3, 26</sup> (the details of the parameter estimation will be published separately). Table 2 lists the values of rate constants obtained by parameter estimation. Remarkably,  $k_p = 8.94 \times 10^8 \text{ l mol}^{-1}\text{sec}^{-1}$  was obtained, which is very close to values measured by

Table 2: Values of rate constants obtained by parameter estimation

Rate constant	Value
$k_0 (\text{l mol}^{-1}\text{sec}^{-1})$	$9.3 \times 10^7$
$k_{-0} (\text{sec}^{-1})$	$3.95 \times 10^7$
$k_1 (\text{l mol}^{-1}\text{sec}^{-1})$	$5.69 \times 10^{-2}$
$k_{-1} (\text{sec}^{-1})$	$3.90 \times 10^7$
$k_2 (\text{l mol}^{-1}\text{sec}^{-1})$	$8.12 \times 10^{-1}$
$k_{-2} (\text{sec}^{-1})$	$3.89 \times 10^7$
$k_p (\text{l mol}^{-1}\text{sec}^{-1})$	$8.94 \times 10^8$

diffusion clock/competition experiments and in irradiation-initiated IB polymerization (Table 1). The capping rate constants  $k_{-0}$ ,  $k_{-1}$  and  $k_{-2}$  were nearly identical ( $3.95$ ,  $3.90$  and  $3.89 \times 10^7 \text{ sec}^{-1}$ ) and were also very close to experimentally measured capping rate constants. Schlaad *et al.* reported  $k_{-1} = 5 \times 10^7 \text{ sec}^{-1}$  and  $k_{-2} = 5 \times 10^7 \text{ sec}^{-1}$ , and  $k_1 = 6.5 \text{ L}^2 \text{ mol}^{-2} \text{ sec}^{-1}$   $k_2 = 16.4 \text{ L}^2 \text{ mol}^{-2} \text{ sec}^{-1}$  (see Scheme 6)<sup>10, 14</sup>. The values of  $k_p/k_{-1} = 16.4$  and  $k_i/k_{-1} = 6.5 \text{ L/mol}$  were obtained using

TMPCl and a PIB 36-mer as initiators, thus  $k_p \approx 3 k_i$ .

Since all rate constants were not available with the models shown in Schemes 3,4 and 5, Predici simulations were carried out using the model in Scheme 1 with the parameters listed in Table 2. Figures 1 and 2 demonstrate very good agreement between simulation and experimental data both for Paths A and B.

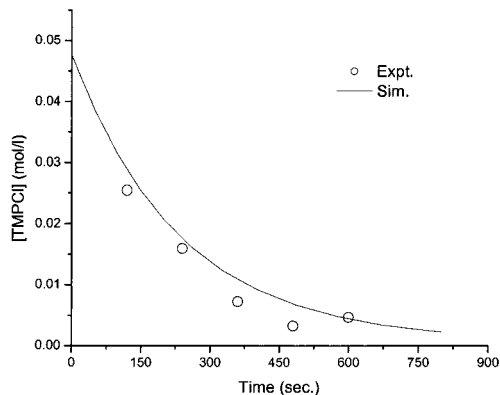


Figure 1. Comparison of predicted and experimental initiator consumption data in living IB polymerization. Path A.

$[TMPCl]_0 = 0.050$  mol/l,  $[TiCl_4]_0 = 0.025$  mol/l,  $[IB]_0 = 2$  mol/l,  $[DtBP]_0 = 0.007$  mol/l, Hx/MeCl=60/40 v/v,  $T = -80^\circ C$ .

Simulation:  $k_0 = 9.3 \times 10^7$  l mol<sup>-1</sup>sec<sup>-1</sup>,  $k_{-0} = 3.95 \times 10^7$  sec<sup>-1</sup>,  $k_1 = 5.69 \times 10^{-2}$  l mol<sup>-1</sup>.sec<sup>-1</sup>,  $k_{-1} = 3.9 \times 10^7$  sec<sup>-1</sup>,  $k_2 = 8.12$  l.mol<sup>-1</sup>.sec<sup>-1</sup>,  $k_{-2} = 3.89 \times 10^7$  sec<sup>-1</sup>,  $k_p = 6 \times 10^8$  l.mol<sup>-1</sup>.sec<sup>-1</sup>.

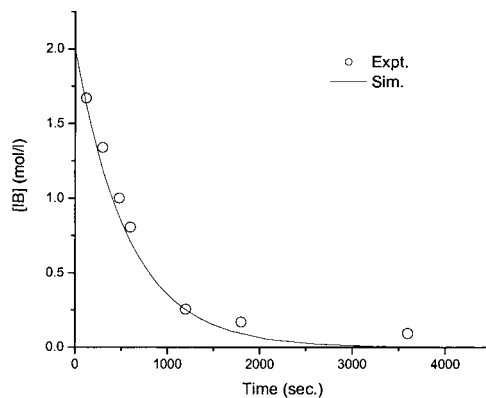


Figure 2. Comparison of predicted and experimental monomer consumption data in living IB polymerization. Path B.

$[\text{TMPCl}]_0 = 0.004 \text{ mol/l}$ ,  $[\text{TiCl}_4]_0 = 0.064 \text{ mol/l}$ ,  $[\text{IB}]_0 = 2 \text{ mol/l}$ ,  $[\text{DtBP}]_0 = 0.007 \text{ mol/l}$ ,  $\text{Hx/MeCl} = 60/40 \text{ v/v}$ ,  $T: -80^\circ\text{C}$

Simulation:  $k_0 = 9.3 \times 10^7 \text{ l mol}^{-1} \text{ sec}^{-1}$ ,  $k_{-0} = 3.95 \times 10^7 \text{ sec}^{-1}$ ,  $k_1 = 5.69 \times 10^{-2} \text{ l mol}^{-1} \text{ sec}^{-1}$ ,  $k_{-1} = 3.9 \times 10^7 \text{ sec}^{-1}$ ,  $k_2 = 8.12 \text{ l mol}^{-1} \text{ sec}^{-1}$ ,  $k_{-2} = 3.89 \times 10^7 \text{ sec}^{-1}$ ,  $k_p = 6 \times 10^8 \text{ l mol}^{-1} \text{ sec}^{-1}$ .

Simulation was also carried out with the model shown in Scheme 6. Figure 3 shows that good fit with experimental data can be obtained with  $k_p = 3 \times 10^7 \text{ l mol}^{-1} \text{ sec}^{-1}$ , but  $k_p = 7 \times 10^8 \text{ l mol}^{-1} \text{ sec}^{-1}$  leads to too fast propagation.

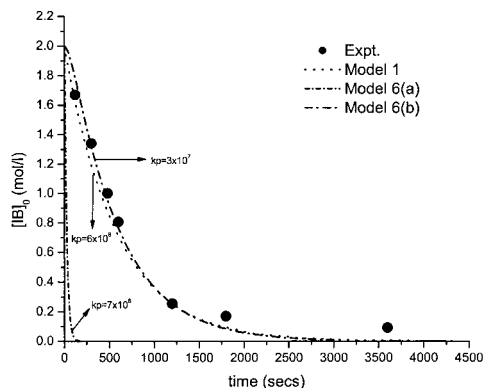


Figure 3. Comparison of predicted and experimental monomer consumption data in living IB polymerization. Path B.

$[\text{TMPCl}]_0 = 0.004 \text{ mol/l}$ ,  $[\text{TiCl}_4]_0 = 0.064 \text{ mol/l}$ ,  $[\text{IB}]_0 = 2 \text{ mol/l}$ ,  $[\text{DtBP}]_0 = 0.007 \text{ mol/l}$ ,  $\text{Hx/MeCl} = 60/40 \text{ v/v}$ ,  $T: -80^\circ\text{C}$

Simulation: Model 1:  $k_0 = 9.3 \times 10^7 \text{ l.mol}^{-1}\text{sec}^{-1}$ ,  $k_{-0} = 3.95 \times 10^7 \text{ sec}^{-1}$ ,  $k_1 = 5.69 \times 10^{-2} \text{ l.mol}^{-1}\text{sec}^{-1}$ ,  $k_{-1} = 3.9 \times 10^7 \text{ sec}^{-1}$ ,  $k_2 = 8.12 \text{ l.mol}^{-1}\text{sec}^{-1}$ ,  $k_{-2} = 3.89 \times 10^7 \text{ sec}^{-1}$ ,  $k_p = 6 \times 10^8 \text{ l.mol}^{-1}\text{sec}^{-1}$ ; Model 6:  $k_1 = 6.5 \text{ l.mol}^{-1}\text{sec}^{-1}$ ,  $k_{-1} = 5 \times 10^7 \text{ sec}^{-1}$ ,  $k_2 = 16.4 \text{ l.mol}^{-1}\text{sec}^{-1}$ ,  $k_{-2} = 3.4 \times 10^7 \text{ sec}^{-1}$ ,  $k_p = 7 \times 10^8$  for Model 6(a) and  $3 \times 10^7 \text{ l.mol}^{-1}\text{sec}^{-1}$  for model 6(b).

The good fits demonstrate that various mechanistic models can fit the same experimental data, thus achieving good match between experimental and simulated data alone cannot be used to prove any mechanistic models. Independent experiments are crucial to establish the mechanistic pathways. In the case of living IB polymerization independent experiments demonstrated  $\text{TiCl}_4$  orders shifting between 1 and 2, depending on experimental conditions. It should be mentioned here that the model in Scheme 5 would dictate propagation predominantly by active centres possessing monomeric counteranions as  $k_p \gg k_D$ . This is in direct contradiction with the authors' experimental data.

The Puskas model also reconciles the discrepancy between  $k_p$  data published for IB polymerizations<sup>14, 17, 18-23</sup>. The lower values ( $10^{4-5} \text{ L/molsec}$ ) were obtained from kinetic measurements that would yield composite rate constants including the pre-equilibrium, while the close to diffusion limited ( $k_p \cong 10^8 \text{ l/mol}^{-1}\text{sec}^{-1}$ ) values were obtained by diffusion clock

methods that yield the true rate constants<sup>17, 14</sup>. For instance, the rate constant obtained by Marek<sup>18</sup> (Table 1) used the assumption that  $[P^+] = [AlBr_3]_0$ , thus the rate equation would read as follows:

$$\frac{-d[M]}{dt} = k_p[P^+][M] = k_p[LA]_0[M] \quad (2)$$

Thus the initial slope of the  $\ln ([M]_0/[M])/[LA]_0$  plot yielded  $k_p$ . In comparison, the rate equation using Model 1 can be written as follows:

$$\frac{-d[M]}{dt} = k_p[P^+][M] = k_p[I]_0[LA]_0^2[M] \quad (\text{Path B}) \quad (3)$$

and the initial slope of the  $\ln ([M]_0/[M])/[LA]_0$  plot would now be  $k_p[I]_0[LA]_0$ . Considering the usual initiator concentration of  $10^{-3}$  mol/l and  $TiCl_4$  concentration of  $10^{-2}$  mol/l in living IB polymerizations could explain the several order of magnitude difference in  $k_p$  measured by the diffusion clock method or kinetic measurements. In addition, complexation between initiator and Lewis acid, or monomer and Lewis acid suggested earlier<sup>18-22, 24</sup> could also influence kinetically obtained rate constants. Remarkably, irradiation-initiated IB polymerization in bulk with no coinitiator<sup>23</sup> yielded  $k_p = 1.4 \times 10^8 \text{ l.mol}^{-1}.\text{sec}^{-1}$ .

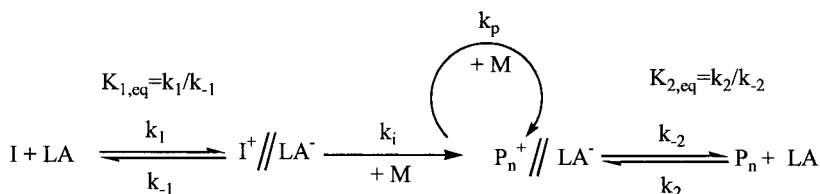
### Kinetics of carbocationic St polymerization initiated by TMPCl/TiCl<sub>4</sub>

Several research groups have investigated the kinetics and mechanism of carbocationic St polymerizations. Polymerizations initiated with TMPCl are most important, since this reaction mimicks blocking St with living PIB in polyisobutylene-polystyrene (PIB-PS) block copolymer synthesis. In contrast to living IB polymerization, in the case of St polymerization initiated by TMPCl/TiCl<sub>4</sub> the structure of the initiator and the growing chain is different, thus  $k_i \neq k_p$ . Indeed, slow initiation was invariably reported in this system. Kaszas *et al.* achieved living St polymerization in the presence of very strong electron pair donors (EDs) such as hexamethylene phosphoramidate, or in the combined presence of N,N-dimethyl acetamide (DMA) as ED and 2,6-di-*tert.*-butylpyridine (DtBP) as a proton trap. Carbocation stabilization by EDs was claimed to be the reason for the living conditions<sup>27</sup>. Majoros and Nagy from the Kennedy group analyzed experimental data of St polymerization initiated with TMPCl/TiCl<sub>4</sub> using the model shown in Scheme 2<sup>4</sup>. The rate of initiation was found to increase with increasing  $[TiCl_4]_0$ , and 100%

initiation efficiency was reached. However, chain transfer to monomer was present and prevented the synthesis of controlled high MW PS. The relatively broad MWD was attributed to slow initiation. Fodor *et al.* from the Faust group reported that living conditions could be achieved in the sole presence of D<sub>t</sub>BP, although initiation was slow<sup>28</sup>. Chain-chain coupling by intermolecular alkylation was avoided by quenching the reactions prior to complete monomer conversion. MWDs were rather broad. The reaction order in terms of TiCl<sub>4</sub> was found to be 2. Storey *et al.* reported that St polymerization with the TMPCl/TiCl<sub>4</sub> system proceeds with slow initiation<sup>29</sup>.

The fact that  $k_i \neq k_p$  further complicates the already complex mechanism shown in Scheme 1, and simplification is needed. In the simple model shown in Scheme 2, only three parameters ( $k_p$ ,  $k_i$  and  $k_1$ ) are needed. However,  $k_1$  would represent a composite “rate constant” which includes [TiCl<sub>4</sub>]<sub>0</sub> and  $K_0$  as well as depicted in Scheme 1. The simplified model was used to simulate IB polymerizations, with the understanding that  $k_1$  was dependent on [TiCl<sub>4</sub>]<sub>0</sub> and good agreement was found with experimental data<sup>7</sup>.

For St polymerization, the simplified scheme (Scheme 7) is shown below:



Scheme 7: Simple model of living St polymerization.

$K_{1\text{eq}} = k_1/k_{-1}$  and  $K_{2\text{eq}} = k_2/k_{-2}$  are apparent equilibrium constants and  $k_i$  and  $k_p$  are the initiation and propagation rate constants, respectively. In the St polymerization experiments, we used D<sub>t</sub>BP as proton trap and DMA as a strong donor to prevent nucleophilic substitution of the St rings. The concentration of these additives was kept constant. It is known that these additives lower the polymerization rate<sup>8,11,27</sup>. However, their presence at a constant concentration would not interfere with our investigation of the effect of [TiCl<sub>4</sub>] and [IB] on the polymerization rate. The effect of temperature also needs to be addressed here. It is very difficult to ensure isothermal condition in carbocationic polymerizations, even at high dilution. The effect of temperature on the rate of polymerization would manifest itself in non-linear semilogarithmic monomer consumption rates.

The St polymerizations in this study showed linear rate plots both in Path A and B, shown in Figures 4 and 5:

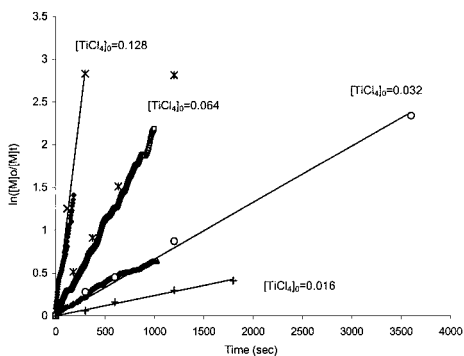


Figure 4.  $\ln [M]_0/[M]$  vs time plots in  $\text{TMPCl}/\text{TiCl}_4$  initiated St polymerization at  $-75^\circ\text{C}$ . Path B.  $[\text{TMPCl}]_0=0.004$  mol/l,  $[\text{DMA}]=0.002$  mol/l,  $[\text{DzBP}]=0.007$  mol/l,  $[\text{St}]_0=2$  mol/l,  $\text{MeCHx}/\text{MeCl}=60/40$  (v/v) FTIR: based on  $-\text{CH}_2=\text{C}-\text{H}$  wagging vibration at  $1690\text{ cm}^{-1}$ .

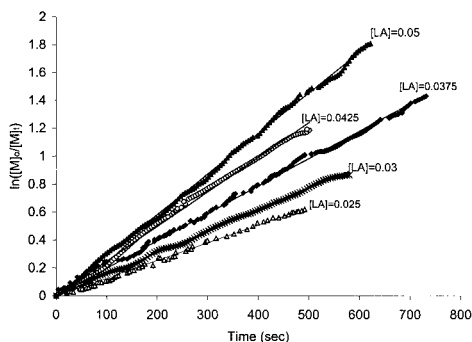


Figure 5.  $\ln [M]_0/[M]$  vs time plots in  $\text{TMPCl}/\text{TiCl}_4$  initiated St polymerization at  $-75^\circ\text{C}$ . Path A.  $[\text{TMPCl}]_0=0.05$  mol/l,  $[\text{St}]_0=2$  mol/l,  $[\text{DMA}]=0.002$  mol/l,  $[\text{DzBP}]=0.007$  mol/l,  $\text{MeCHx}/\text{MeCl}=60/40$  (v/v) FTIR: based on  $-\text{CH}_2=\text{C}-\text{H}$  wagging vibration at  $1690\text{ cm}^{-1}$ .

Figures 4 and 5 demonstrate that non-isothermal conditions did not effect the polymerization rate. This can be explained as follows: when the dormant-active equilibrium is strongly shifted and the steady-state approximation  $d([I^+] + [P_n^+])/dt \approx 0$  can be evoked, and  $[I] + [P_n] = [I]$ , the rate will be

directly proportional to  $[I]_0$  and  $[LA]_0$ , in spite of changing  $[I]$  and  $[P_n]$ . This was shown by gravimetry in living IB polymerization<sup>12</sup>, and in living vinyl ether polymerization.<sup>30</sup> Another approach to achieve Path A and reduce the exotherm would be to simply reduce the  $[TiCl_4]$  concentration. We attempted this with  $[TMPCl]_0 = 0.004$  mol/l. However, we could not find appropriate conditions and at  $[TiCl_4]_0 = 0.02$  mol/l polymerization stopped completely as we reached the DMA concentration.

In contrast to IB polymerization, initiator consumption data can be obtained in both Path A and B since initiation is slow in Path B as well. The experimental  $\ln [I]_0/[I]$  plots were not linear. Thus the kinetics of initiation were evaluated using the initial rate method, which is recommended for systems with unknown mechanism<sup>31</sup>.

### *Kinetics of Initiation*

Using the simplified model in Scheme 7, the initiator consumption can be written as follows:

$$\frac{-d[I]}{dt} = k_1[I][LA] - k_{-1}[I^+] \quad (4)$$

Since  $K_1$  is very small and  $k_1 \ll k_i$ ,<sup>7, 12</sup> the steady-state approximation can be used:

$$\frac{d[I^+]}{dt} = k_1[I][LA] - k_{-i}[I^+][M] - k_{-1}[I^+] \cong 0$$

$$\frac{d[I^+]}{dt} = k_1[I][LA] - k_{-i}[I^+][M] - k_{-1}[I^+] \cong 0 \quad (5)$$

$$\text{Therefore from (5), } [I^+] = \frac{k_1[I][LA]}{k_i[M] + k_{-1}} \quad (6)$$

Substituting (6) into (4) we get



$$\frac{-d[I]}{dt} = \frac{k_1[I][LA] \frac{k_i}{k_{-1}}[M]}{1 + \frac{k_i}{k_{-1}}[M]} \quad (7)$$

For living IB polymerizations initiated by TMPCl,  $k_i \approx k_p$ , thus

$$\frac{k_i}{k_{-1}}[M] \gg 1$$

and

$$\ln \frac{[I]_0}{[I]} = k_1[LA]_0 t \quad (8)$$

The rate of initiator consumption was found to be directly proportional to  $k_1$  and  $[\text{TiCl}_4]_0^{3,12}$  and  $k_1 = 0.22 \text{ l mol}^{-1} \text{ sec}^{-1}$  was obtained from experimental initiator consumption data<sup>3</sup>. For St polymerization using TMPCl as initiator  $k_i \ll k_{-1}$  can be assumed. This is a reasonable assumption since  $k_{-1} \approx 3.9 \times 10^7 \text{ l/mol sec}^{11}$  and slow initiation was reported by several authors for the TMPCl/TiCl<sub>4</sub>/St system<sup>4, 27-29</sup>. Thus

$$\frac{k_i}{k_{-1}}[M] \ll 1$$

and

$$\frac{-d[I]}{dt} = \frac{k_1 k_i}{k_{-1}} [I][LA][M] \quad (9)$$

Thus, based on kinetic derivation, in the case of St polymerization the rate of initiator consumption will depend not only on  $[\text{TiCl}_4]_0$  but  $[M]$  as well. This was proven experimentally, as shown in Figure 6. Simply increasing  $[M]_0$  from 0.5 to 2.0 M increased the initiator efficiency from 20% to 100% when the conversion reached about 80% conversion.

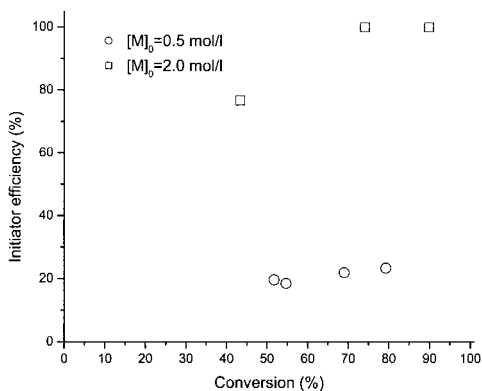


Figure 6. Effect of  $[St]_0$  on  $I_{eff}$  in polymerizations initiated by  $TMPCl/TiCl_4$ .  $[TMPCl]_0=0.004$  mol/l,  $[TiCl_4]_0=0.04$  mol/l,  $[DMA]=0.002$  mol/l,  $[DtBP]=0.007$  mol/l,  $MeCHx/MeCl=60/40$ ,  $T=-75^\circ C$ .

Equation (6) can be integrated analytically for low conversion where  $[M] \approx [M]_0$

$$\ln \frac{[I]_0}{[I]} = k_{i,app} [LA]_0 [M]_0 t \quad (10)$$

$$\text{where } k_{i,app} = \frac{k_1 k_i}{k_{-1}}$$

Thus  $k_{i,app}$  data were obtained from the initial slope of experimental initiator consumption plots. In carbocationic St polymerizations initiated by  $TMPCl/TiCl_4/DMA$  slow initiation was found not only at  $[TMPCl]_0 > [TiCl_4]_0$ , but also at  $[TMPCl]_0 < [TiCl_4]_0$  with relatively low  $[TiCl_4]_0$  as shown in Figure 7.

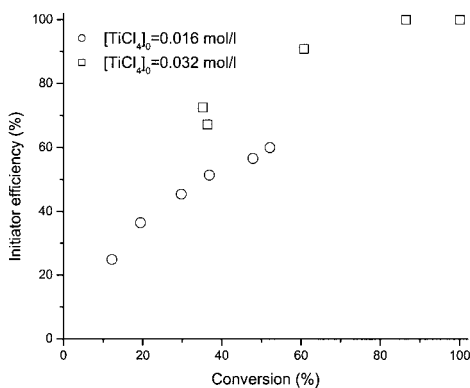


Figure 7. Slow initiation in carbocationic St polymerizations initiated by TMPCl/TiCl<sub>4</sub>. Path B. [TMPCl]<sub>0</sub>=0.004 mol/l, [St]<sub>0</sub>=2 mol/l [DMA]=0.002 mol/l, [DtBP]=0.007 mol/l MeCHx/MeCl=60/40, T= -75<sup>0</sup>C.

The initial slope of the  $\ln[I]_0/[I]$  plots,  $[d[I]/dt]_0$ , was obtained from the nonlinear initiator consumption plots and the values are listed in Table 3.

Table 3:  $k_{i,app}$  values in carbocationic St polymerizations initiated by TMPCl/TiCl<sub>4</sub>. [St]<sub>0</sub>=2 mol/l [DMA]=0.002 mol/l, [DtBP]=0.007 mol/l MeCHx/MeCl=60/40, T= -75<sup>0</sup>C

[I] <sub>0</sub> mol/l	[TiCl <sub>4</sub> ] <sub>0</sub> mol/l	(d[I]/dt) <sub>0</sub>	$k_{i,app}$ l <sup>2</sup> mol <sup>-2</sup> s <sup>-1</sup>
0.05	0.050	0.125	1.25
0.05	0.030	0.092	1.53
0.05	0.025	0.077	1.55
0.05	0.013	0.035	1.39
0.004	0.016	0.040	1.23

It can be seen that  $k_{i,app}$  values are independent of [TiCl<sub>4</sub>]<sub>0</sub>, indicating that initiation is first order in TiCl<sub>4</sub>. Interestingly, Storey *et al.* found similar values ( $k_i$ = 1.3 l<sup>2</sup>mol<sup>-2</sup>s<sup>-1</sup>) using the rapid monomer consumption (RMC) technique<sup>32</sup>. The TiCl<sub>4</sub> order was also obtained from the dependence of the initial rate on [TiCl]<sub>0</sub>:

$$\left(\frac{d[I]}{dt}\right)_0 = k_{i,app} [TiCl_4]_0^n \quad (11)$$

$$\ln\left(\frac{d[I]}{dt}\right)_0 = \ln k_{i,app} + n \ln[TiCl_4]_0 \quad (12)$$

where  $k_{i,app}$  is an apparent rate constant. The  $\ln(d[I]/dt)_0$  vs  $\ln[TiCl_4]_0$  plot was linear, with a slope of  $n = 0.98$ , verifying first order. This finding is similar to the living IB system<sup>3</sup>. The kinetic treatment presented here may be applicable to other polymerizations governed by dormant-active equilibria<sup>33</sup>.

### *Kinetics of Propagation*

The  $TiCl_4$  order of propagation was investigated by varying the  $TiCl_4$  concentration, while keeping all other variables constant, as discussed above:

$$\ln\left(\frac{d[M]}{dt}\right)_0 = \ln k_{p,app} + n \ln[TiCl_4]_0 \quad (13)$$

where  $k_{p,app}$  is an apparent rate constant lumping all the other variables. In case of a complex reaction several variables may influence the rate and hence the reaction order. These may be factors such as complex formation between products (for instance, the complex forming between  $TiCl_4$  and DMA), the difference between  $K_i$  and  $K_{eq}$ , or even nonisothermal conditions. The initial rate method is designed to circumvent these effects and will yield correct order data. The accuracy of the data will depend on the accuracy of initial rate measurements, which are greatly improved with *in-situ* FTIR monitoring methods<sup>5</sup>. Both *in-situ* FTIR and gravimetric analysis were used in our experiments. Figures 4 and 5 show that the plots are linear, so the initial slope method does not have to be used. Figure 8 shows  $\ln(k_{p,app})$  values obtained from the slopes of the lines in Figure 4, versus  $\ln[TiCl_4]_0$ . The  $TiCl_4$  order is  $n = 1.83$ , similar to that reported for living IB polymerizations<sup>3, 7</sup>.

Figure 8 shows FTIR linear rate plots for St polymerizations conducted with excess  $\text{TiCl}_4$  over  $\text{TMPCl}$  (Path A). The reaction was relatively fast and therefore gravimetry was not conducted. Conditions were not isothermal, but this did not seem to effect polymerization rates. Figure 9 shows the order plot.

From Figure 9, the  $\text{TiCl}_4$  reaction order is 1.2. This finding indicates that, similarly to IB polymerization initiated by  $\text{TMPCl}/\text{TiCl}_4$ , the reaction order is closer to 1 at  $[\text{TMPCl}]_0/[\text{TiCl}_4]_0 \geq 1$ .

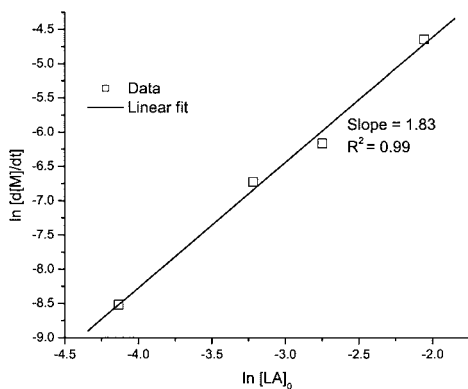


Figure 8.  $\ln (k_{p,app})$  vs  $\ln[\text{TiCl}_4]_0$  plot for  $[\text{TiCl}_4]_0 > [\text{TMPCl}]_0$  in  $\text{TMPCl}/\text{TiCl}_4$  initiated St polymerization at  $-75^\circ\text{C}$ .  $[\text{TMPCl}]_0=0.004$  mol/l,  $[\text{St}]_0=2$  mol/l,  $[\text{DMA}]=0.002$  mol/l,  $[\text{DzBP}]=0.007$  mol/l,  $\text{MeCHx}/\text{MeCl}=60/40$  (v/v).

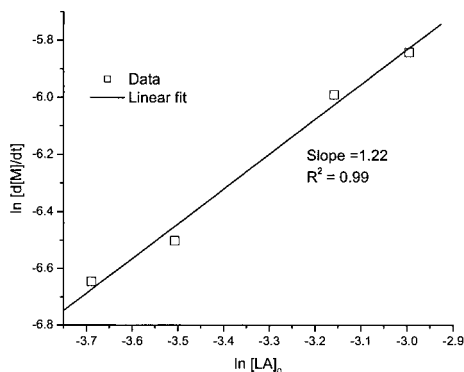


Figure 9.  $\ln(k_{p,app})$  vs  $\ln[LA]_0$  plot for  $[LA]_0 \leq [I]_0$  in TMPCl/TiCl<sub>4</sub> initiated St polymerization at -75°C.  $[TMPCl]_0=0.05$  mol/l,  $[St]_0=2$  mol/l,  $[DMA]=0.002$  mol/l,  $[DtBP]=0.007$  mol/l, MeCHx/MeCl=60/40 (v/v).

In summary, the carbocationic polymerization of St initiated by the TMPCl/TiCl<sub>4</sub>/DMA system was found to be a complex reaction. Analysis of kinetic data showed that the rate of initiation is directly proportional to  $[TiCl_4]_0$  and  $[M]$ , and  $k_{i,app}$  values were obtained. The polymerization reaction order with respect to  $[TiCl_4]_0$  was found to be 1.83 at  $[TMPCl]_0/[TiCl_4]_0 < 1$  and 1.2 at  $[TMPCl]_0/[TiCl_4]_0 > 1$ . Judicious selection of the reaction conditions led to living conditions; living polymerization was achieved at  $[TMPCl]_0 = 0.004$  mol/L and  $[TiCl_4]_0 = 0.032 - 0.064$  mol/L, yielding high MW PS ( $M_n = 45,000$  g/mol). High  $[TiCl_4]$  (0.128 M) led to alkylation, but only after the monomer was depleted as shown in Figure 10.

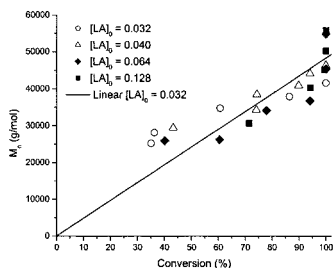


Figure 10.  $[TMPCl]_0=0.004$  mol/l,  $[St]_0=2$  mol/l,  $[DMA]=0.002$ mol/l,  $[DtBP]=0.007$ mol/l MeCHx/MeCl=60/40, T= -75°C.

## Conclusion

In conclusion, living carbocationic IB and St polymerizations exhibited similar kinetic behaviour. The rate of initiation was first order in  $\text{TiCl}_4$  in both systems, but was shown to be also dependent on  $[\text{St}]_0$  – in this system initiation was slow. The rate of propagation was found to be closer to first order in  $\text{TiCl}_4$  at  $[\text{TiCl}_4]_0 < [\text{TMPCl}]_0$  and followed a close to second order in  $\text{TiCl}_4$  at  $[\text{TiCl}_4]_0 \geq [\text{TMPCl}]_0$ . By optimization of polymerization conditions, high molecular weight PS was produced at a high initiator efficiency.

## Acknowledgement

The authors would like to thank W. Luo and A. Naskar for their contribution to this work. Financial support from NSERC (Canada) and Bayer Polymers (Bayer Inc., Canada) is also acknowledged.

- [1] J. P. Kennedy, *J. Polym. Sci., Part A: Polym. Chem.* **1999**, 37, 2285
- [2] J. E. Puskas, G. Kaszas, *Prog. Polym. Sci.* **2000**; 25, 403
- [3] J. E. Puskas, M. G. Lanzendörfer, *Macromolecules* **1998**; 31, 8684
- [4] I. Majoros, A. Nagy, J. P. Kennedy. *Adv. Polym. Sci.* **1994**, 112, 1
- [5] J. E. Puskas *et al.*, in “*In Situ Monitoring of Monomer and Polymer Synthesis*”, J. E. Puskas, T. E. Long, R. F. Storey, Eds., Kluwer Academic/Plenum Pub., **2003**, p.37
- [6] C. Paulo, J. E. Puskas, S. Angepat, *Macromolecules* **2000**, 33, 4634
- [7] J. E. Puskas, H. Peng, *Polym. React. Eng.* **1999**, 7(4), 553
- [8] R. F. Storey, K. R. Choate Jr., *Macromolecules* **1997**, 30, 4799
- [9] Y. Wu, Y. Tan, G. Wu, *Macromolecules* **2002**, 35, 3801
- [10] H. Schlaad, Y. Kwon, R. Faust, H. Mayr, *Macromolecules* **2000**, 33, 743
- [11] R. F. Storey, A. B. Donnalley, *Macromolecules* **2000**, 33, 53
- [12] G. Kaszas, J. E. Puskas, *Polym. React. Eng.* **1994**; 2(3), 251
- [13] J. E. Puskas, G. Kaszas, M. Litt *Macromolecules* **1991**, 24, 5278
- [14] H. Schlaad, Y. Kwon, L. Sipos, R. Faust, B Charleaux *Macromolecules* **2000**, 33, 8225
- [15] H. Schlaad, K. Erentova, R. Faust, B Charleaux, M Moreau, J. P. Vairon, H. Mayr *Macromolecules* **1998**, 31, 8058
- [16] A.H.E.Müller, G.Litvinenko, D. Yan, *Macromolecules* **1996**, 29, 2339
- [17] M. Roth, H. Mayr, *Macromolecules* **1996**, 29, 6104
- [18] M. Marek, M. Chmelir, *J. Polym Sci.* **1967**, 22, 177
- [19] L. Toman, M. Marek, *Makromol. Chem.* **1976**, 22, 3325
- [20] P. L. Magagnini, S. Cesca; P. Giusti, A. Priola, M. Di Maina, *Makromol. Chem.*, **1977**, 178, 2235
- [21] K. Ueno, H Yamaoka, K. Hayashi, S. Okamura, *Int. J. Appl. Radiat. Isotopes*, **1966**, 17, 595
- [22] P. H. Plesch, *Prog. Reaction Kinetics* **1993**, 18, 1
- [23] R. B. Taylor, F. Williams, *J. Am. Chem. Soc.*, **1969**, C22, 177
- [24] P. H. Plesch, *Macromolecules* **2001**, 34, 1143
- [25] Wulkow, M. PREDICI®, *Simulation Package for Polyreactions*, Ver. 5.18.5, CiT GmbH, **2001**
- [26] S. Shaikh, H. Peng, J. E. Puskas, *Polym. Prepr.* **2002**, 43(1), 260
- [27] G. Kaszas, J. E. Puskas, J. P. Kennedy, W. G. Hager. *J. Polym. Sci., Part A: Polym. Chem.* **1991**, 29, 421

- [28] Z. S. Fodor, M. Györ, H. Wang, R. Faust, *J. Macromol. Sci., Pure Appl. Chem.* **1993**, A30(5), 349
- [29] R. F. Storey, S. J. Jeskey, *Polym Prepr.* **2000**, 41(2), 1895
- [30] M. Kamigaito, K. Yamaoka, M. Sawamoto, T. Higashimura, *Macromolecules* **1992**, 25, 6400
- [31] O. Levenspiel, "*Chemical Reaction Engineering*", 3rd ed., J. Wiley & Sons, New York, 1999
- [32] R. F. Storey, Q. A. Thomas, *Macromolecules* **2003**, 36, 5065
- [33] J. E. Puskas, W. Luo, *Macromolecules* **2003**, 36, 6942